Fluid theory of magnetic-field generation in intense laser-plasma interaction

EUROPHYSICS LETTERS 15 December 2005

Europhys. Lett., **72** (6), pp. 955–961 (2005)
DOI: 10.1209/epl/i2005-10329-2

Fluid theory of magnetic-field generation in intense laser-plasma interaction

Bin Qiao[1], X. T. He[2,3] and Shao-ping Zhu[2]

[1] *Graduate School of China Academy of Engineering Physics*
P. O. Box 2101, Beijing 100088, PRC
[2] *Institute of Applied Physics and Computational Mathematics*
P. O. Box 8009, Beijing 100088, PRC
[3] *Department of Physics, Zhejiang University - Hangzhou 310027, PRC*

received 11 July 2005; accepted in final form 14 October 2005
published online 16 November 2005

PACS. 52.38.Fz – Laser-induced magnetic fields in plasmas.
PACS. 52.35.Mw – Nonlinear phenomena: waves, wave propagation, and other interactions (including parametric effects, mode coupling, ponderomotive effects etc.).
PACS. 52.57.Kk – Fast ignition of compressed fusion fuels.

Abstract. – Using the ten-moment Grad system of hydrodynamic equations, a self-consistent fluid model is presented for the generation of spontaneous magnetic fields in intense laser-plasma interaction. The generalized vorticity is not conserved as opposed to previous studies, for the nondiagonal stress force is considered. Equations for both the axial magnetic field B_z and the azimuthal one B_θ are simultaneously derived from a fluid scheme for the first time in the quasi-static approximation, where the low-frequency phase speed v_p is much smaller than the electron thermal speed v_{te}. It is found that the condition $v_p \gg v_{te}$, widely used as cold-fluid approximation, where B_z is incomplete, is improper. The profiles of B_z and B_θ as well as the plasma density cavitation are analyzed. Their dependences on the laser intensity are also discussed.

In the study of the interaction of an intense short-pulse laser with relativistic plasma [1], the generation of spontaneous magnetic fields is most significant because these fields have considerable influence on the whole nonlinear plasma dynamics. The study of this problem has wide applications in the fast-ignition scheme [2] and particle acceleration. Although much effort [3–7] has been done, there still exists a great deal of controversy concerning the proper derivation for the spontaneous magnetic fields. It has been argued in refs. [8, 9] that only a kinetic treatment can give the correct expression and that all fluid attempts yield unsatisfactory results. So far, no fluid model can give complete spontaneous magnetic fields including the axial component B_z and the azimuthal one B_θ, as in the kinetic theory [9–12].

We believe some facts should be noted during the self-consistent derivation of spontaneous magnetic fields. 1) In intense laser-plasma interaction, there exist strong rotational motions (currents) and large vortexes are generated, thus the fluid viscosity force (the nondiagonal stress tensor) should be considered. Ideal-fluid assumption in most studies is improper. 2) In this case, the generalized vorticity is not conserved as opposed to previous ideal-fluid models [5, 13]. 3) With intense laser, the plasma is warmed and the condition $v_p \gg v_{te}$ (v_p is the low-frequency phase speed and v_{te} the electron thermal speed) widely used as cold-fluid approximation [5, 13] is improper. The condition $v_p \ll v_{te}$ in the quasi-static approximation should be satisfied.

In this paper, we consider an intense laser propagating in an initially uniform plasma. Ion motion and the excitation of Langmuir waves are ignored. The electron motion can be

well described by the ten-moment Grad system of hydrodynamic equations [14, 15], which is a closed system of equations providing an approximate solution to the Boltzmann equation and is composed of ten independent components of variables including density n, momentum $\boldsymbol{p}_i$ and stress tensor $\boldsymbol{\Pi}_{ij}$. We give the system of equations as

$$\frac{\partial \boldsymbol{p}_i}{\partial t} + \boldsymbol{v}\cdot\nabla \boldsymbol{p}_i = -e\left[\boldsymbol{E} + \frac{1}{c}(\boldsymbol{v}\times\boldsymbol{B})\right]_i + \frac{\partial \boldsymbol{\Pi}_{ij}}{\partial r_j}, \tag{1}$$

$$\frac{\partial \boldsymbol{\Pi}_{ij}}{\partial t} + \frac{\partial}{\partial r_s}(\boldsymbol{u}_s\boldsymbol{\Pi}_{ij}) + \boldsymbol{\Pi}_{is}\frac{\partial \boldsymbol{u}_j}{\partial r_s} + \boldsymbol{\Pi}_{js}\frac{\partial \boldsymbol{u}_i}{\partial r_s} - \frac{2}{3}\delta_{ij}\boldsymbol{\Pi}_{sl}\frac{\partial \boldsymbol{u}_l}{\partial r_s} + \\ + \frac{e}{mc}\boldsymbol{B}_l(e_{isl}\boldsymbol{\Pi}_{js} + e_{jsl}\boldsymbol{\Pi}_{is}) = v_{te}^2\left(\frac{\partial \boldsymbol{p}_i}{\partial r_j} + \frac{\partial \boldsymbol{p}_j}{\partial r_i} - \frac{2}{3}\delta_{ij}\nabla\cdot\boldsymbol{p}\right), \tag{2}$$

where the electric field $\boldsymbol{E}$ and magnetic field $\boldsymbol{B}$ are governed by Maxwell equations as

$$\nabla\times\boldsymbol{E} = -\frac{1}{c}\frac{\partial \boldsymbol{B}}{\partial t}, \tag{3}$$

$$\nabla\times\boldsymbol{B} = \frac{1}{c}\frac{\partial \boldsymbol{E}}{\partial t} + \frac{4\pi}{c}\boldsymbol{j} = \frac{1}{c}\frac{\partial \boldsymbol{E}}{\partial t} - \frac{4\pi e}{c}n\boldsymbol{v}, \tag{4}$$

$$\nabla\cdot\boldsymbol{E} = 4\pi(n_0 - n)e. \tag{5}$$

Here $-e$, m, n and $v_{te} = \sqrt{T_e/m}$ represent the charge, mass, density and thermal velocity of electrons. n_0 is the initial density. $\boldsymbol{p}_i = \gamma m\boldsymbol{v}_i$ is the electron momentum and $\gamma_i = (1+\boldsymbol{p}_i^2/m^2c^2)^{1/2}$ is the relativistic factor. The stress tensor is written as $\boldsymbol{\Pi}_{ij} = \frac{1}{n_0}m\sigma_{ij}$, where the diagonal components represent the normal pressure $P_{ij} = \delta_{ij}mn_0T_e$ and the nondiagonal components represent the viscosity force. For the incompressible plasma electron fluid, defining the stress force as $\boldsymbol{F}_i = \frac{\partial \boldsymbol{\Pi}_{ij}}{\partial r_j}$, eq. (2) can be much simplified as $\frac{\partial \boldsymbol{F}_i}{\partial t} = \frac{1}{\gamma}v_t^2\nabla^2\boldsymbol{p}_i - \frac{iv_t^2}{4\omega_0 m\gamma^2}\nabla^2\nabla\times(\boldsymbol{p}_i\times\boldsymbol{p}_i)$.

Now we divide both electron motion and fields into slow- and fast-time-scale parts as $\boldsymbol{p} = \langle\boldsymbol{p}\rangle + \frac{1}{2}\tilde{\boldsymbol{p}}e^{-i\omega_0 t} + \frac{1}{2}\tilde{\boldsymbol{p}}^* e^{i\omega_0 t}$, $\boldsymbol{E} = \langle\boldsymbol{E}\rangle + \frac{1}{2}\tilde{\boldsymbol{E}}e^{-i\omega_0 t} + \frac{1}{2}\tilde{\boldsymbol{E}}^* e^{i\omega_0 t}$ and $\boldsymbol{B} = \langle\boldsymbol{B}\rangle + \frac{1}{2}\tilde{\boldsymbol{B}}e^{-i\omega_0 t} + \frac{1}{2}\tilde{\boldsymbol{B}}^* e^{i\omega_0 t}$, where the angular bracket $\langle\ \rangle$ denotes averaging over the fast time period $(2\pi/\omega_0)$ and $*$ denotes the complex conjugate for the fast-time-scale parts. Here and below, the subscript i is and will be not written for simplification. Note that here $\langle\boldsymbol{B}\rangle$ just represents the spontaneous magnetic field, and $\tilde{\boldsymbol{E}}$ represents the laser electric field. Introducing the generalized vorticity $\Omega \equiv \nabla\times\boldsymbol{p} - \frac{e}{c}\boldsymbol{B}$ and splitting Ω similarly, the slow-time-scale parts of eqs. (1), (2), (4) can be simplified as

$$\frac{\partial\langle\boldsymbol{p}\rangle}{\partial t} = -e\langle\boldsymbol{E}\rangle - \frac{1}{4m\gamma}\nabla\langle\tilde{\boldsymbol{p}}\cdot\tilde{\boldsymbol{p}}^*\rangle + \frac{1}{4m\gamma}\langle\tilde{\boldsymbol{p}}\times\tilde{\boldsymbol{\Omega}}^* + \tilde{\boldsymbol{p}}^*\times\tilde{\boldsymbol{\Omega}}\rangle + \langle\boldsymbol{F}\rangle, \tag{6}$$

$$\frac{\partial\langle\boldsymbol{F}\rangle}{\partial t} = \frac{1}{\gamma}v_t^2\nabla^2\langle\boldsymbol{p}\rangle - \frac{iv_t^2}{4\omega_0 m\gamma^2}\nabla^2\nabla\times\langle\tilde{\boldsymbol{p}}\times\tilde{\boldsymbol{p}}^*\rangle, \tag{7}$$

$$\nabla\times\langle\boldsymbol{B}\rangle = \frac{1}{c}\frac{\partial\langle\boldsymbol{E}\rangle}{\partial t} - \frac{4\pi e}{m\gamma c}\langle n\rangle\langle\boldsymbol{p}\rangle - \frac{\pi e}{m\gamma c}\langle\tilde{n}\tilde{\boldsymbol{p}}^* + \tilde{n}^*\tilde{\boldsymbol{p}}\rangle, \tag{8}$$

where $\langle\gamma\rangle = \gamma$ is assumed. Applying the curl operator on eq. (6) and using eq. (3), we get

$$\frac{\partial\langle\boldsymbol{\Omega}\rangle}{\partial t} = \frac{1}{4m\gamma}\nabla\times\langle\tilde{\boldsymbol{p}}\times\tilde{\boldsymbol{\Omega}}^* + \tilde{\boldsymbol{p}}^*\times\tilde{\boldsymbol{\Omega}}\rangle + \nabla\times\langle\boldsymbol{F}\rangle. \tag{9}$$

From eq. (9), we can see the generalized vorticity $\langle\boldsymbol{\Omega}\rangle$ is not conserved and is generated by the nondiagonal stress force due to nonzero electron thermal motion in plasmas. From eqs. (6)-(9), after some calculation, we obtain the equation for $\langle\boldsymbol{p}\rangle$ in the lowest order as

$$c^2\nabla\times\nabla\times\langle\boldsymbol{p}\rangle+\frac{\partial^2\langle\boldsymbol{p}\rangle}{\partial t^2}+\frac{1}{4m\gamma}\frac{\partial}{\partial t}\nabla\langle\boldsymbol{p}\cdot\boldsymbol{p}^*\rangle+\omega_{pe}^2\frac{\langle n\rangle}{n_0}\frac{\langle\boldsymbol{p}\rangle}{\gamma}-\frac{v_{te}^2}{\gamma}\nabla^2\langle\boldsymbol{p}\rangle-c^2\nabla\times\langle\boldsymbol{\Omega}\rangle=$$
$$=-\frac{\omega_{pe}^2}{4n_0\gamma}\langle\tilde{n}\tilde{\boldsymbol{p}}^*+\tilde{n}^*\tilde{\boldsymbol{p}}\rangle-i\frac{v_{te}^2}{4m\omega_0\gamma^2}\nabla^2\nabla\times\langle\tilde{\boldsymbol{p}}\times\tilde{\boldsymbol{p}}^*\rangle,\quad(10)$$

where $\omega_{pe}=\sqrt{4\pi n_0e^2/m}$ is defined. Note eq. (10) includes the generalized vorticity $\langle\boldsymbol{\Omega}\rangle$.

Similarly, to the lowest order, for $\omega_0\gg v_{te}\nabla$, we get fast-time-scale quantities, respectively, as $\tilde{\boldsymbol{p}}=-\frac{ie}{\omega_0}\tilde{\boldsymbol{E}}$, $\tilde{\boldsymbol{F}}=\frac{ev_{te}^2}{\gamma\omega_0^2}\nabla^2\tilde{\boldsymbol{E}}$, $\tilde{\boldsymbol{\Omega}}=0$. Using the continuity equation $\frac{\partial n}{\partial t}+\nabla\cdot(n\frac{\boldsymbol{p}}{m\gamma})=0$, we get

$$\langle\tilde{n}\tilde{\boldsymbol{p}}^*+\tilde{n}^*\tilde{\boldsymbol{p}}\rangle=i\frac{e^2}{m\omega_0^3}\tilde{\boldsymbol{E}}\nabla\cdot\frac{\langle n\rangle\tilde{\boldsymbol{E}}^*}{\gamma}+\text{c.c.}\quad(11)$$

Making a second differential for eq. (10) related to t, getting $\frac{\partial^2\langle\boldsymbol{\Omega}\rangle}{\partial t^2}$ from eqs. (7), (9) and then substituting $\frac{\partial^2\langle\boldsymbol{\Omega}\rangle}{\partial t^2}$ and eq. (11) into it, we obtain the coupling equation for $\langle\boldsymbol{p}\rangle$ as

$$\frac{\partial^2}{\partial t^2}\left[c^2\nabla\times\nabla\times\langle\boldsymbol{p}\rangle+\frac{\partial^2\langle\boldsymbol{p}\rangle}{\partial t^2}+\omega_{pe}^2\frac{\langle n\rangle}{n_0}\frac{\langle\boldsymbol{p}\rangle}{\gamma}+\frac{e^2}{4m\omega_0^2\gamma}\frac{\partial}{\partial t}\nabla\langle\boldsymbol{E}\cdot\boldsymbol{E}^*\rangle+\right.$$
$$\left.+\frac{\omega_{pe}^2e^2}{4mn_0\omega_0^3}\left(\frac{i\tilde{\boldsymbol{E}}}{\gamma}\nabla\cdot\frac{\langle n\rangle\tilde{\boldsymbol{E}}^*}{\gamma}+\text{c.c.}\right)\right]-\frac{\partial^2}{\partial t^2}\left[\frac{v_{te}^2}{\gamma}\nabla^2\langle\boldsymbol{p}\rangle-i\frac{v_{te}^2e^2}{4m\omega_0^3\gamma^2}\nabla^2\nabla\times\langle\tilde{\boldsymbol{E}}\times\tilde{\boldsymbol{E}}^*\rangle\right]=$$
$$=c^2\frac{v_{te}^2}{\gamma}\nabla^2\nabla\times\left[\langle\boldsymbol{p}\rangle-\frac{ie^2}{4m\omega_0^3\gamma}\nabla\times\langle\tilde{\boldsymbol{E}}\times\tilde{\boldsymbol{E}}^*\rangle\right].\quad(12)$$

From eq. (12), we can see that the relation between v_{te} and the low-frequency phase speed $v_p=\frac{\omega_s}{q}$ (ω_s is the frequency, and q the wave number) is a key condition, for $\frac{\partial}{\partial t}=\omega_s$ and $v_{te}\nabla=v_{te}q$ here.

In intense laser-plasma interaction, the plasma electron is warmed and v_{te} cannot be approximately regarded as zero anylonger. Thus, the previous widely used condition $v_p\gg v_{te}$ for the cold-fluid approximation [5, 13] is not satisfied anylonger. Note here that the low frequency ω_s is indeed a beat frequency of two high frequencies (ω_1, ω_2), as $\omega_s=\omega_1-\omega_2$. In the quasi-static approximation, it is reasonable to assume that ω_2 is very close to ω_1 and both of them are close to ω_0. Thus, ω_s is much smaller than the characteristic oscillating frequency of plasma electrons ω_{pe}, which is determined by v_{te} as $\omega_{pe}=v_{te}/\lambda_{De}$ (λ_{De} is the electron Debye length) and has the same scale as ω_0. When the spatial scale $\frac{1}{q}$ of the low-frequency field is comparable to or smaller than λ_{De}, the condition $v_p\ll v_{te}$ is always satisfied. In fact, the beat frequency ω_s is approximately equivalent to the ion-acoustic frequency, *i.e.*, $\omega_s=qv_s=q\sqrt{\frac{T_e}{m_i}}$ (m_i is the ion mass) and thus $v_p=v_s\ll v_{te}$ is always satisfied.

Under the condition $v_p\ll v_{te}$ for quasi-static approximation, the right-hand side of eq. (12) is dominant, the left-hand side can be ignored as zero, thus from eq. (12), we get

$$\langle\boldsymbol{p}\rangle=\frac{ie^2}{4m\omega_0^3\gamma}\nabla\times\langle\tilde{\boldsymbol{E}}\times\tilde{\boldsymbol{E}}^*\rangle.\quad(13)$$

Substituting eqs. (11), (13) into eq. (8), ignoring $\frac{\partial\langle E\rangle}{\partial t}$ due to $\frac{\partial}{\partial t}\ll v_{te}\nabla$, we get $\langle\boldsymbol{B}\rangle$ as

$$\nabla\times\langle\boldsymbol{B}\rangle=-i\frac{\omega_{pe}^2e}{4m\omega_0^3c\gamma^2}\frac{\langle n\rangle}{n_0}\nabla\times\langle\tilde{\boldsymbol{E}}\times\tilde{\boldsymbol{E}}^*\rangle-\frac{\omega_{pe}^2e}{4m\omega_0^3c}\left(\frac{i\tilde{\boldsymbol{E}}}{\gamma}\nabla\cdot\frac{\langle n\rangle\tilde{\boldsymbol{E}}^*}{n_0\gamma}+\text{c.c.}\right).\quad(14)$$

Substituting eq. (13) into eq. (7) and making its divergence, we get $\frac{\partial\nabla\cdot\boldsymbol{F}}{\partial t}=0$, *i.e.*, $\nabla\cdot\boldsymbol{F}=0$. Thus, from eqs. (5), (6), we get the slow-time-scale plasma density $\frac{\langle n\rangle}{n_0}$ as

$$\frac{\langle n\rangle}{n_0} = 1 + \frac{e^2}{4m^2\omega_{pe}^2\omega_0^2\gamma}\nabla^2\langle\tilde{\boldsymbol{E}}\cdot\tilde{\boldsymbol{E}}^*\rangle. \tag{15}$$

Equation (14) combined with eq. (15) together gives the axial spontaneous magnetic fields and their two driven sources. The first source is the rotational current as the result of the beating interaction high-frequency electromagnetic waves (laser wave fields) $\langle\tilde{\boldsymbol{E}}\times\tilde{\boldsymbol{E}}^*\rangle$, the second one is the rotational current as the result of the coupling interaction between the high-frequency electron quiver velocity and the high-frequency electron density perturbation (see eq. (14)). Note such two sources are unitedly and simultaneously given for the first time. In most of the previous fluid models [5, 13], the viscosity force is not considered and the cold-fluid approximation $v_p \gg v_{te}$ is improperly used, which leads to the absence of the first source and the incomplete axial magnetic field. From eqs. (13), (14), we can also prove that the generalized vorticity is not conserved when the viscosity force is considered, as opposed to previous ideal-fluid models [5, 13]. The generated vorticity induced by high-frequency fields is $\nabla\times\langle\boldsymbol{\Omega}\rangle = \frac{e^2}{4m\omega_0^3\gamma}[i\frac{\omega_{pe}^2}{c^2\gamma}\frac{\langle n\rangle}{n_0}\nabla\times\langle\tilde{\boldsymbol{E}}\times\tilde{\boldsymbol{E}}^*\rangle + \frac{\omega_{pe}^2}{c^2}(i\tilde{\boldsymbol{E}}\nabla\cdot\frac{\langle n\rangle\tilde{\boldsymbol{E}}^*}{n_0\gamma} + \text{c.c.}) - i\nabla^2\nabla\times\langle\tilde{\boldsymbol{E}}\times\tilde{\boldsymbol{E}}^*\rangle]$. Another fact that should be noted is that the inverse Faraday effect is included in our model. Let us apply the curl operator on eq. (6), noticing that $\tilde{\boldsymbol{\Omega}} = 0$ and $\nabla\times\langle\boldsymbol{p}\rangle = \langle\boldsymbol{\Omega}\rangle + \frac{e}{c}\langle\boldsymbol{B}\rangle$ and considering eq. (9), we easily get $\frac{\partial\langle\boldsymbol{B}\rangle}{\partial t} = -c\nabla\times\langle\boldsymbol{E}\rangle$, which is just the equation describing the inverse Faraday effect.

For simplicity, now we consider the interaction of an underdense plasma with an intense laser. We assume that the laser beam propagates along the z-axis direction with wave number $k_0 = \frac{2\pi}{\lambda_0}$, under the Coulomb gauge, the electric fields are usually expressed as $\boldsymbol{E}_L(\boldsymbol{x},t) = \frac{1}{2}E_0(r,t)(\boldsymbol{e}_r + i\alpha\boldsymbol{e}_\theta)e^{i\alpha\theta}e^{ik_0z-i\omega_0t} + \text{c.c.}$, where $\alpha = 0, \pm1$ for linearly polarized (LP) and circularly polarized (CP) laser, respectively. The laser intensity is assumed to have Gaussian distribution $I = I_0e^{-r^2/r_0^2-(z-ct)^2/L^2}$ and $E_0 = \sqrt{I}$, where L is the pulse longitudinal width, and r_0 the transverse radius. Thus the above high-frequency electric field is expressed as $\tilde{\boldsymbol{E}} = E_0(r,t)(\boldsymbol{e}_r + i\alpha\boldsymbol{e}_\theta)e^{i\alpha\theta}e^{ik_0z}$ and $\gamma = (1+\frac{\boldsymbol{P}^2}{m^2c^2})^{1/2} = [1+\frac{(1+\alpha^2)e^2E_0^2}{2m^2c^2\omega^2}]^{1/2} = [1+\frac{(1+\alpha^2)}{2.76}I_0\lambda_{\mu m}^2e^{-r^2/r_0^2-(z-ct)^2/L^2}]^{1/2}$ is obtained. Introducing the normalized transform $t\to\frac{t}{\omega_0}, \boldsymbol{x}\to\frac{c\boldsymbol{x}}{\omega_0}, E\to E\frac{m_ec\omega_0}{e}, B\to B\frac{m_ec\omega_0}{e}$, using B_z to represent $\langle B_z\rangle$ and noticing that $\nabla\cdot\tilde{\boldsymbol{E}}\simeq 0$ is satisfied for a laser beam propagating in an underdense plasma (see ref. [12]), we get the normalized B_z from eqs. (14),(15),

$$\frac{\partial B_z}{\partial r} = -\frac{\alpha}{1+\alpha^2}n_0\frac{1}{\gamma}\frac{\partial}{\partial r}\left(\frac{\langle n\rangle}{n_0}\frac{\gamma^2-1}{\gamma}\right), \tag{16}$$

where

$$\frac{\langle n\rangle}{n_0} = 1 - \frac{1}{n_0r_0^2}\frac{\gamma^2-1}{\gamma}\left(2 - \frac{r^2}{r_0^2}\frac{\gamma^2+1}{\gamma^2}\right). \tag{17}$$

Equation (16) shows that B_z is only generated by CP laser ($\alpha=\pm1$). For LP laser ($\alpha=0$), B_z is zero.

The transverse profile of $|B_z|$ calculated by eqs. (16), (17) is plotted in fig. 1(a), where the laser intensity is $I_0 = 10^{19}\,\text{W/cm}^2$ with wavelength $\lambda = 1.05\,\mu\text{m}$, the transverse focused radii are, respectively, $r_0 = 1\lambda,\ 2\lambda,\ 3\lambda$. The plasma density is $n_0 = 0.36n_{cr}$. The parameters are consistent with those after focusing on the 3D particle simulation of ref. [12]. It can be seen that B_z dominates the "inner" zone near the laser axis and the peak $|B_z|$ is about 20–26 MG at the axis for $r_0 = 1$–3λ. Either the profile or the peak value of $|B_z|$ is very close to the simulation results [12]. Recent experiment [16] reports that a B_z of about 2 MG is generated by CP laser with "vacuum" $I_0 = 6.7\times10^{18}\,\text{W/cm}^2$ and "vacuum" $r_0 = 10\lambda$ ($\lambda = 1.05\,\mu\text{m}$), where $n_0 = 2.8\times10^{19}\,\text{cm}^{-3}$. Using equations (16), (17), $|B_z| \sim 1.93\,\text{MG}$ is estimated under the same

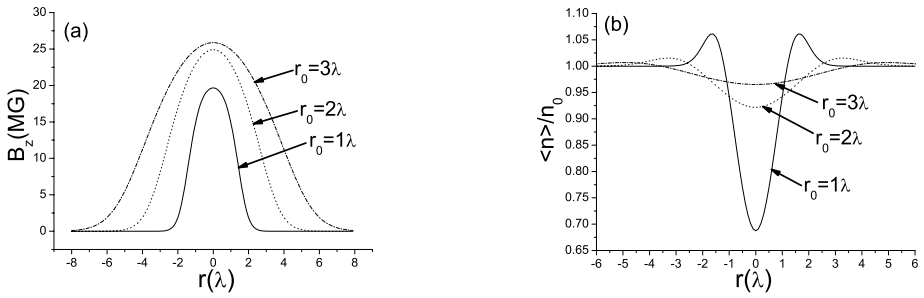

Fig. 1 – The transverse profiles of (a) the axial magnetic field B_z and (b) the plasma density cavitation $\langle n\rangle/n_0$ as a function of the radius r calculated by eqs. (16), (17), for a Gaussian laser beam with intensity $I_0 = 10^{19}\,\mathrm{W/cm^2}$, wavelength $\lambda = 1.05\,\mu$m, and transverse radii $r_0 = 1\lambda,\ 2\lambda,\ 3\lambda$. The plasma density is $n_0 = 0.36 n_{cr}$.

parameters, where we assume I_0 be two times the "vacuum" laser intensity and r_0 decreased down to 5λ, due to self-focusing. The result is also very close to that in experiment [16].

Figure 1(b) plots the transverse profile of plasma density $\langle n\rangle/n_0$ by eq. (17) for the same parameters as fig. 1(a). We can evidently see that electrons in the region $r < r_0$ are expelled by the ponderomotive force so that $\langle n\rangle/n_0 < 1$, and the expelled electrons will be deposited at a cavity edge with $r \succeq r_0$, where $\langle n\rangle/n_0 > 1$; then when $r \gg r_0$, $\langle n\rangle/n_0 = 1$ is taken again.

The experimental results of [16] show that B_z increases with laser intensity I_0. Figure 2 plots the dependences of $|B_z|$ and $\frac{\langle n\rangle}{n_0}$ on I_0, where other parameters are consistent with those in fig. 1. It can be seen that the peak $|B_z|$ increases with I_0, while the plasma density near the axis $(\frac{\langle n\rangle}{n_0})_{r=0}$ decreases as I_0 increases. When I_0 rises high enough, the peak B_z does not increase anymore. However, in a dense plasma, the fields can be quite strong for high-intensity laser. Indeed, for $I_0 = 4\times10^{20}\,\mathrm{W/cm^2}$ ($\lambda = 1.05\,\mu$m), and $n_0 = 0.9\times10^{21}\,\mathrm{cm^{-3}}$, B_z turns out to be 150 MG.

The above analysis is only for the azimuthal momentum $\langle P_\theta\rangle$, which generates B_z. For the azimuthal magnetic field B_θ, the longitudinal momentum $\langle p_z\rangle$ should be studied. For the same Gaussian laser beam propagating in an underdense plasma as above, from eq. (12), assuming $\frac{\partial\langle p_r\rangle}{\partial z} \ll \frac{\partial\langle p_z\rangle}{\partial r}$, we get the normalized coupling equation of $\langle p_z\rangle$ as

$$\frac{\partial^2\langle p_z\rangle}{\partial\xi^2} - \frac{\partial^2\langle p_z\rangle}{\partial r^2} - \frac{1}{r}\frac{\partial\langle p_z\rangle}{\partial r} + n_0\frac{\langle n\rangle}{n_0\gamma}\langle p_z\rangle = \frac{1}{4\gamma}\frac{\partial^2\langle\tilde{\boldsymbol{E}}\cdot\tilde{\boldsymbol{E}}^*\rangle}{\partial\xi^2} = \frac{\partial^2\gamma}{\partial\xi^2}, \tag{18}$$

where $\xi = z - t$ is taken. Notice that B_θ is mainly produced by the longitudinal current,

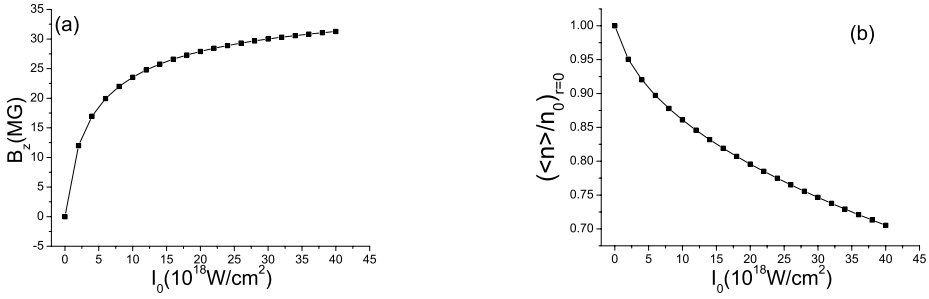

Fig. 2 – The dependence of the peak B_z (a) and $\langle n\rangle/n_0$ at the axis ($r = 0$) (b) on the laser intensity I_0, where the transverse radius r_0 is taken equal to 1.5λ and the other parameters are consistent with fig. 1.

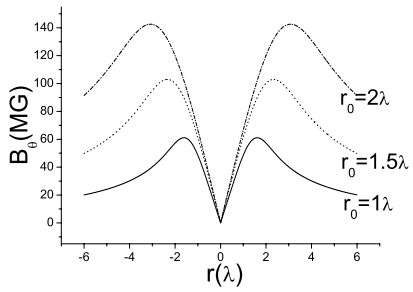

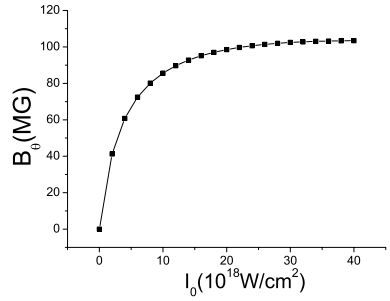

Fig. 3 – The transverse profiles of the azimuthal magnetic field B_θ calculated by eq. (19) with the same parameters as in fig. 1, except for r_0 which is taken as 1λ, 1.5λ, and 2λ, respectively.

Fig. 4 – The dependence of the peak B_θ on the laser intensity I_0, where the laser beam transverse radius r_0 is taken equal to 1.5λ and the other parameters are consistent with fig. 1.

which dominates near the axis. That is to say, B_θ is mainly decided by p_z near the axis. Thus, it is reasonable to ignore $\frac{\partial\langle p_z\rangle}{\partial r}$ and $n_0\frac{\langle n\rangle}{n_0\gamma}\langle p_z\rangle$ in eq. (18) and then eq. (18) is simplified as $\frac{\partial^2\langle p_z\rangle}{\partial\xi^2} = \frac{\partial^2\gamma}{\partial\xi^2}$. Assuming initially $\gamma = 1$ when $\langle p_z\rangle = 0$, then we obtain that $\langle p_z\rangle = \gamma - 1$.

Ignoring $\frac{\partial\langle \boldsymbol{E}\rangle}{\partial t}$, using the symbol B_θ to represent $\langle B_\theta\rangle$, from eq. (8), we get the normalized B_θ as

$$\frac{1}{r}\frac{\partial}{\partial r}(rB_\theta) = -n_0\frac{\langle n\rangle}{n_0}\frac{\gamma-1}{\gamma}. \tag{19}$$

Equation (19) shows that both the CP laser ($\alpha = \pm 1$) and LP laser ($\alpha = 0$) can generate B_θ.

The transverse profile of $|B_\theta|$ by eq. (19) is plotted in fig. 3, where the parameters are consistent with those of fig. 1, except for r_0, which is taken as 1λ, 1.5λ, and 2λ, respectively. It can be seen that B_θ dominates the "outer" zone away from the laser axis, is close to zero near the axis, increases gradually with r until it reaches its peak value at about $r = r_0$, then decreases due to return currents. The peak B_θ at $r = r_0$ is about 60–140 MG for $r_0 = 1$–2λ. The results and the profile are both close to the particle simulation [12]. Experiment [17] reports that $B_\theta \sim 35$–70 MG is produced by LP laser with "vacuum" $I_0 = 4.7\times10^{18}\,\mathrm{W/cm^2}$ and $r_0 = 4\lambda$ ($\lambda = 1.05\,\mu$m), where $n_0 = 2\times10^{20}\,\mathrm{cm^{-3}}$. We also assume that the focused I_0 is two times its "vacuum" value as $I_0 = 9.4\times10^{18}\,\mathrm{W/cm^2}$ and the focused $r_0 = 1.5\lambda$ due to self-focusing. Using eq. (19), the peak B_θ is estimated to be about 52 MG, which agrees well with the experimental result of [17]. Figure 4 plots the dependence of B_θ on the laser intensity I_0, where $r_0 = 1.5\lambda$ and the other parameters are the same as in fig. 1. It shows that the peak $|B_\theta|$ also increases with laser intensity I_0.

Recently, observations of nearly Giga-Gauss (GG) B_θ generated in ultra-intense laser overdense plasma interaction are reported by Tatarakis *et al.* [18] and Wagner *et al.* [19], which can be explained by the scaling law of Sudan [3]. As mentioned in refs. [18, 19], the minimum B_θ should be generated at the nonrelativistic critical density surface ($n_0 \simeq n_{cr}$), the higher B_θ should be generated in the higher density region ($n_{cr} < n_0 < \gamma n_{cr}$) due to laser hole-boring. For the same parameters as those of the experiments, *i.e.*, $I_0 = 9\times10^{19}\,\mathrm{W/cm^2}$ and $\lambda = 1.05\,\mu$m, assuming that the Gaussian distribution of laser intensity is still valid for $n_0 < \gamma n_{cr} = 6n_{cr}$, we can calculate B_θ by our model too. Using eq. (19), peaks $B_\theta = 360$ MG, 466 MG, 795 MG (0.36 GG, 0.47 GG, 0.79 GG) are estimated, respectively, at densities $n_0 = 0.95n_{cr}, 1.2n_{cr}, 2.4n_{cr}$, which are close to the experimental results of [18,19]. Certainly, this is a rough estimate, for the laser hole-boring effect is a very complex topic.

In conclusion, a self-consistent fluid model is presented for the spontaneous magnetic fields including the axial part B_z and the azimuthal one B_θ generated by an intense CP and LP laser propagating in an initially uniform plasma. The ten-moment Grad system of hydrodynamic equations is used, where the nondiagonal stress tensor (the fluid viscosity force) is taken into account, for there exist strong rotational motions (vortexes) in intense laser warm plasma interaction. The generalized vorticity is proved to be not conserved, as opposed to previous studies with ideal-fluid assumption. This hydrodynamic derivation yields exact and complete expressions for both B_z and B_θ for the first time. In the quasi-static approximation $v_p \ll v_{te}$, B_z is driven by two rotational currents generated only by CP laser, one is the result of the beating interaction of the high-frequency electric fields of CP laser, and the other is the result of the coupling interaction between the high-frequency electron quiver velocity and the high-frequency electron density perturbation. These two sources are simultaneously given for the first time. B_θ is driven by the irrotational current of ponderomotive force. It is shown that the condition $v_p \gg v_{te}$, widely used as cold-fluid approximation in previous studies, where the first source of B_z is not given and B_z is incomplete, is improper. The results calculated by our model are compared with those of the particle simulation of ref. [12] and with the experiments [16–19]. The transverse profiles of both B_z and B_θ as well as the plasma density cavitation $\langle n \rangle / n_0$ are analyzed. Their dependences on the laser intensity are also discussed.

* * *

This work was supported by National Hi-Tech ICF Committee of China, NSFC Grant No. 10335020, 10375011 and 10135010, National Basic Research Project "nonlinear Science".

REFERENCES

[1] BORISOV A. B. *et al.*, *Phys. Rev. Lett.*, **68** (1992) 2309; WILKS S. C. *et al.*, *Phys. Rev. Lett.*, **69** (1992) 1383; HONDA M. *et al.*, *Phys. Plasmas*, **7** (2000) 1302.
[2] TABAK M. *et al.*, *Phys. Plasmas*, **1** (1994) 1626.
[3] SUDAN R. N., *Phys. Rev. Lett.*, **70** (1993) 3075; LEHNER T., *Phys. Scr.*, **49** (1994) 704.
[4] SHENG Z. M. and MEYER-TER-VEHN J., *Phys. Rev. E.*, **54** (1996) 1833.
[5] BEREZHIANI V. I., MAHAJAN S. M. and SHATASHVILI N. L., *Phys. Rev. E.*, **55** (1997) 995.
[6] HAINES G., *Phys. Rev. Lett.*, **87** (2001) 135005.
[7] KIM A., TUSHENTSOV M., ANDERSON D. and LISAK M., *Phys. Rev. Lett.*, **89** (2002) 095003.
[8] ŜKORIĆ M. M., *Laser Part. Beams*, **5** (1987) 83.
[9] BEREZHIANI V. I., TSKHAKAYA D. D. and AUER G., *J. Plasma Phys.*, **38** (1987) 139.
[10] BEZZERIDES B. *et al.*, *Phys. Rev. Lett.*, **38** (1977) 495; MORA P. and PELLAT R., *Phys. Fluids*, **22** (1979) 2408; KONO M., *et al.*, *Phys. Lett. A*, **77** (1980) 27.
[11] ZHU SHAO-PING, HE X. T. and ZHENG C. Y., *Phys. Plasmas*, **8** (2001) 312.
[12] QIAO BIN, ZHU SHAO-PING, ZHENG C. Y. and HE X. T., *Phys. Plasmas*, **12** (2005) 053104.
[13] GORBUNOV L. M., *Usp. Fiz. Nauk*, **109** (631) 1973 (*Sov. Phys. Usp.*, **16** (1973) 217); TSINTSADZE N. L. *et al.*, *Zh. Eksp. Teor. Fiz.*, **72** (1977) 48016 (*Sov. Phys. JETP*, **45** (1977) 252).
[14] GRAD H., *Commun. Pure Appl. Math.*, **2** (1949) 331; KIRII A. YU. *et al.*, *Zh. Tekh. Fiz.*, **39** (1969) 773 (*Sov. Phys. Tech. Phys.*, **14** (1969) 583); ALEXANDER N. GORBAN *et al.*, *Phys. Rev. E*, **54** (1996) R3109.
[15] ALIEV YU. M., FROLOV A. A. and STENFLO L. *et al.*, *Phys. Fluids B*, **2** (1990) 34.
[16] NAJMUDIN Z., TATARAKIS M. *et al.*, *Phys. Rev. Lett.*, **87** (2001) 215004-1.
[17] FUCHS J., MALKA G. *et al.*, *Phys. Rev. Lett.*, **80** (1998) 1658.
[18] TATARAKIS M. *et al.*, *Nature*, **415** (2002) 280; *Phys. Plasmas*, **9** (2002) 2244.
[19] U. WAGNER, *Phys. Rev. E*, **70** (2004) 026401.